

THRUSTER PLACEMENT ISSUES AND POSSIBLE MITIGATION METHODS FOR THE ST-7 DISTURBANCE REDUCTION SYSTEM

O. C. Hsu, P. G. Maghami, F. L. Markley, and M. B. Houghton
NASA Goddard Space Flight Center
Mission Engineering and Systems Analysis Division
Greenbelt, MD 20771

ABSTRACT

The Space Technology-7 Disturbance Reduction System is being designed to demonstrate the ability to shield a test mass from non-gravitational forces. In order to meet this goal, two advanced technologies will be employed: a highly sensitive Gravitational Reference Sensor and micro-Newton thrusters. ST-7 is limited to two clusters of four thrusters, which are sufficient to provide control for 6 degrees of freedom, but the overall effectiveness of the baseline configuration is limited by the noise on the measurement signals and the thrust outputs, the disturbance force caused by solar radiation pressure, and the performance of the individual thrusters. This paper presents and discusses these issues in greater detail along with possible mitigation methods.

INTRODUCTION

The Disturbance Reduction System (DRS) has been selected by NASA's New Millennium Program as the key technology advancement of the Space Technology-7 (ST-7) Mission. ST-7 is scheduled for launch in 2007 aboard the European Space Agency's SMART-2 spacecraft in a drift away trajectory towards the Sun-Earth L1 point. The Jet Propulsion Laboratory (JPL) is managing the overall program; and the three other major organizations working on the project are Stanford University, Busek Company, and NASA's Goddard Space Flight Center (GSFC). ST-7 is designed to test two advanced technologies, a highly sensitive Gravitational Reference Sensor (GRS) provided by Stanford University and micro-Newton colloidal thrusters provided by the Busek Company. Goddard Space Flight Center is responsible for the design of the Dynamic Control System (DCS) that interconnects the GRS, star tracker, and micro-Newton thrusters. The primary responsibility of the DCS is to maintain the spacecraft's position with respect to the free-floating test mass to less than $10\text{nm}/\sqrt{\text{Hz}}$ within the science measurement band from 1 mHz to 30 mHz, as well as to provide sun coarse pointing.

This paper discusses the issues that have arisen with the baseline thruster configuration, and it presents the possible mitigation methods. These issues include the thruster variation levels resulting from transforming the commanded spacecraft force and torque into individual thruster firing levels, the DC thrust levels required to counteract the solar radiation pressure force, and the overall control authority available from the two clusters. The variation levels required to meet the performance requirements are hard to achieve with the current hardware requirements and flight assumptions. Possible mitigation methods discussed in this paper include changing thruster placement and orientation, refining the mission requirements, and tightening the capacitive sensing and thruster noise requirements.

MODEL DESCRIPTION

This section provides a general description of the spacecraft and the baseline thruster configuration and the capabilities associated with the configuration. In addition, the primary operation modes of concern to the thruster configuration will be discussed, as well as the primary disturbance source, Solar Radiation Pressure (SRP).

Spacecraft and Thrusters

ST-7 consists of two GRSs and eight micro-Newton thrusters. Each GRS contains a free floating test mass that is used to measure the relative displacement of the GRS housing with respect to the test mass. The test masses within each GRS are located at $\mathbf{R}_1 = [-0.1 \ 0.05 \ 0.3]^T \text{ m}$ and $\mathbf{R}_2 = [0.1 \ 0.05 \ 0.3]^T \text{ m}$ with respect to the spacecraft center of mass in the current analysis model. As a result, the sensitive axis for the current GRS locations is the spacecraft X-axis and the +Z face of the spacecraft points towards the Sun. The geometry can be seen in Figure 2. The masses of the spacecraft and test masses are assumed to be 400 kg and 1.25 kg, respectively.

The current spacecraft baseline assumes that ST-7 can be modeled as an 8-sided spacecraft with two clusters of four micro-Newton thrusters located on the $\pm X$ faces. A perspective view of a thruster cluster is shown in Figure 1. In this figure, the larger cylinders represent the four thrusters that emit positively charged particles. The smaller cylinders are the neutralizers that emit electrons in order to maintain the charge neutrality on the spacecraft. The remainder of the assembly contains the power supply, electronics, and the propellant required to fire all four thrusters at the maximum thrust for the entire ST-7 mission. Each thruster is always firing and is capable of producing a variable thrust force between $2 \mu\text{N}$ and $20 \mu\text{N}$ in $0.1 \mu\text{N}$ increments. The thrusters are able to vary the thrust levels quickly ($t < 100 \text{ msec}$) for thrust changes of $\pm 20\%$ about a set point, and the set point can change between the minimum and maximum thrust levels in 100 seconds. The thruster locations and angle definitions are shown Figure 2, where the azimuth angle is denoted as ϕ_n and measured from the z-axis in the local horizontal, the elevation angle is denoted as θ_n and measured from the Y-Z Plane, and subscript n denotes the thruster number. The azimuth and elevation angle definitions assume that the thruster mounting flange is the local horizontal plane. Subsequently, the thrusters can be subdivided into two groups where the subscript t (top) denotes thrusters 1, 2, 5, and 6, and subscript b (bottom) denotes thrusters 3, 4, 7, and 8.

The baseline configuration has 45° elevation angles, 135° azimuth angle for thrusters 3, 4, 7, and 8, and 45° azimuth angle for thrusters 1, 2, 5, and 6. This configuration can also be identified as the 45-45-135-45 configuration, where the nomenclature is $\phi_t\theta_t\phi_b\theta_b$. From the given azimuth and elevation angle of each thruster, the thruster authority matrix $H_{\text{authority}}$, which resolves the individual thrusts (eight component vector τ in μN) into forces (F in μN) and torques (T in $\mu\text{N-m}$) acting on the spacecraft center of gravity (CG), can be computed as:

$$H_{\text{authority}} = \begin{bmatrix} 0.707 & 0.707 & 0.707 & 0.707 & -0.707 & -0.707 & -0.707 & -0.707 \\ 0.500 & -0.500 & -0.500 & 0.500 & -0.500 & 0.500 & 0.500 & -0.500 \\ -0.500 & -0.500 & 0.500 & 0.500 & -0.500 & -0.500 & 0.500 & 0.500 \\ -0.160 & 0.160 & 0.090 & -0.090 & 0.160 & -0.160 & -0.090 & 0.090 \\ -0.223 & -0.223 & 0.577 & 0.577 & 0.223 & 0.223 & -0.577 & -0.577 \\ -0.450 & 0.450 & 0.450 & -0.450 & -0.450 & 0.450 & 0.450 & -0.450 \end{bmatrix} \quad (1.1)$$

$$\begin{bmatrix} F \\ T \end{bmatrix} = H_{\text{authority}} \tau_{\text{cmd}} \quad (1.2)$$

The authority matrix has rank six, therefore providing control along all six degrees of freedom, and the null space consists of two null vectors: $[1 \ 0 \ 1 \ 0 \ 1 \ 0 \ 1 \ 0]^T$ and $[0 \ 1 \ 0 \ 1 \ 0 \ 1 \ 0 \ 1]^T$. The pseudo inverse of the $H_{\text{authority}}$ matrix, H_{dist} , allows the individual thrust command to be determined from the desired forces and torques and it is defined as:

$$\tau_{\text{cmd}} = H_{\text{dist}} \begin{bmatrix} F_{\text{desired}} \\ T_{\text{desired}} \end{bmatrix} = \begin{bmatrix} 0.255 & -0.634 & -0.250 & -3.536 & -0.313 & -0.278 \\ 0.255 & 0.634 & -0.250 & 3.536 & -0.313 & 0.278 \\ 0.099 & -1.134 & 0.250 & -3.536 & 0.313 & 0.278 \\ 0.099 & 1.134 & 0.250 & 3.536 & 0.313 & -0.278 \\ -0.255 & 0.634 & -0.250 & 3.536 & 0.313 & -0.278 \\ -0.255 & -0.634 & -0.250 & -3.536 & 0.313 & 0.278 \\ -0.099 & 1.134 & 0.250 & 3.536 & -0.313 & 0.278 \\ -0.099 & -1.134 & 0.250 & -3.536 & -0.313 & -0.278 \end{bmatrix} \begin{bmatrix} F_{\text{desired}} \\ T_{\text{desired}} \end{bmatrix} \quad (1.3)$$

The pseudo inverse produces a matrix with both positive and negative thrust levels. However, the thrusters are only capable of producing a positive thrust and therefore, must be biased to produce valid thrust levels. With the bias included, the actual force and torque applied to the spacecraft by the thrusters is defined as:

$$\begin{bmatrix} \mathbf{F}_{actual} \\ \mathbf{T}_{actual} \end{bmatrix} = H_{authority} \left(H_{dist} \begin{bmatrix} \mathbf{F}_{desired} \\ \mathbf{T}_{desired} \end{bmatrix} + \tau_{bias} + \tau_{noise} \right) \quad (1.4)$$

where τ_{noise} is an 8-component noise vector and τ_{bias} is an 8-component vector containing the thruster bias levels.

Based on $H_{authority}$ and H_{dist} , the maximum control authority of the baseline thruster configuration, defined by having a minimum thrust level of 2 μN and a maximum thrust level of 20 μN , is shown in Table 1. Y-Force control authority is much less than the X and Z-Force control authority because the geometry and the location of the thrusters with respect to the center of gravity requires additional thruster firings to counteract the torques produced by the primary thrusters. The low X-Torque control authority is a result of the small moment arms about the X-axis associated with each thruster.

Table 1: Maximum Control Authority for Baseline Configuration

Max. X Force (μN)	± 35.3	Max. X Torque ($\mu\text{N-m}$)	± 2.5
Max. Y Force (μN)	± 7.9	Max. Y Torque ($\mu\text{N-m}$)	± 28.8
Max. Z Force (μN)	± 36.0	Max. Z Torque ($\mu\text{N-m}$)	± 32.4

DCS Operation Modes

The DCS has five primary operation modes where the requirements and set points on the thrusters may differ. The modes of primary concern for thruster placement are the Attitude Only (AO) mode and the Full Drag Free or Science Mode (SM). AO mode requires the DCS to control the spacecraft in attitude only thereby neglecting the acceleration caused by the solar radiation pressure. Unlike AO mode, SM mode requires the DCS to counteract the SRP force while maintaining attitude control and keeping the spacecraft centered about the test masses. Therefore, these two modes bound the capabilities of the thrusters. Within the two modes, three primary factors drive the overall placement of the thrusters: solar radiation pressure force acting on SMART-2, thruster command variation, control authority and noise of the thrusters.

Solar Radiation Pressure

SRP may produce two types of disturbances on the spacecraft: a disturbance torque and disturbance force. The AO mode is only required to counteract the SRP disturbance torque (up to 2 $\mu\text{N-m}$ in any axis) and any rates present during hand-over from the SMART-2 spacecraft. The SM mode is concerned with both the disturbance force and torque, but the spacecraft should be at an equilibrium hold attitude thereby eliminating the disturbance caused by the SRP torque. Therefore, the capability requirements on the thrusters will be different for the two modes.

The projected total SRP force acting on the spacecraft at the Sun-Earth L1 point is approximately 19.0 μN , which is based on the assumptions that the surface area exposed to the sun is planar, entirely composed of solar cells, and has a surface area of 3.14 m^2 . For this analysis, the optical properties of the solar cells are assumed to be 0.238 for the coefficient of specular reflection and 0.042 for the coefficient of diffuse reflection. The mean momentum flux is calculated at Earth's perihelion and scaled to represent the Sun-Earth L1 point. The final assumption is that the sun vector and normal vector from the surface of the solar cells are parallel.

CONCERNS WITH BASELINE CONFIGURATION

There are three concerns that exist with the baseline thruster configuration. They are thruster variation levels, control authority, and thruster noise contribution.

Thruster Variation Level

Individual thruster variation level is a concern because the properties of the thrusters limit nominal thrust changes to $\pm 20\%$ of the current set point within 100 msec, and the minimum to maximum thrust level transition times to 100 seconds. Using the current controller design and a white noise requirement for the capacitive sensing noise, the time histories of the individual thruster variation levels are shown in Figures 3 to Figure 10. From the time history data, thruster #3 has the largest peak to peak variation and the results are summarized in Table 2, where the table shows the percent of points above certain thrust levels and the peak to peak levels for 5 window sizes or sample periods.

Table 2: Summary of Thruster #3 Results

Thrust Level (μN)	Percent of Time above level	Window (sec)	Peak to Peak Level (μN)
± 1.00	3.96	1	2.1
± 1.25	0.95	5	3.5
± 1.50	0.22	10	3.5
± 1.75	0.04	15	3.6
		100	3.6

From the individual time histories, the required thruster variations for the top and bottom thrusters are $\pm 1.7 \mu\text{N}$ and $\pm 1.8 \mu\text{N}$, respectively, where the variation level was based on 20,000 seconds of data collected at 10 Hz. Based on the time history data and the 20% fast thruster variation, thruster set point levels of $8.5 \mu\text{N}$ and $9 \mu\text{N}$ are required, and the thruster levels required to counteract a $19 \mu\text{N}$ SRP force with the baseline thruster configuration are $[8.5 \ 8.5 \ 18 \ 18 \ 8.5 \ 8.5 \ 18 \ 18]^T \mu\text{N}$. Therefore, 20% variation for this configuration allows for thruster variations of $\pm 1.7 \mu\text{N}$ for the top thrusters and $\pm 3.6 \mu\text{N}$ for the bottom thrusters. The variation capability of the thrusters for the baseline configuration is adequate but larger margins would be preferable. Since the majority of the thrust command is below $\pm 1.0 \mu\text{N}$, another possible solution is to clip the thruster variation level or allow the thrusters to saturate and not provide the commanded thrust.

Thruster Control Authority and Noise

Thruster control authority and noise contributions are the other driving factors effecting the thruster orientation and placement on the SMART-2 spacecraft. The requirements on control authority and noise contribution are different for the two primary control modes, AO and SM. As stated previously, AO mode is concerned only with attitude control so the torque capability of the thrusters are of primary concern; and the SM mode is concerned with counteracting the SRP force and shielding the test masses from external disturbances therefore thruster variation capability, overall control authority, and thruster noise contribution are all of concern.

Examining the baseline configuration, the X-torque capability is the weakest degree of freedom, and this is strictly an artifact of the thruster location within the thruster assembly and the azimuth and elevation angles of the individual thrusters. The baseline configuration is capable of counteracting a $\pm 2.5 \mu\text{N-m}$ torque in the X-axis and a greater torque in the other axes. When the force required to counteract the SRP Force is included, the X-torque capability reduces to $\pm 1.2 \mu\text{N-m}$.

The major noise sources that affect the relative position of the test masses are the thruster noise and capacitive sensing noise. Representation root power spectral density plots for test mass 1 are shown in Figures 11 to 13. Due to the constantly firing nature of the thrusters, the thrusters are always injecting noise into the measurement signal. The contribution to each axis for the baseline configuration is shown in Table 3, where the numbers represent the Root Sum Square (RSS) of the individual thruster components upon each axis. This table shows that the noise contribution is highest along the sensitive axis or X-axis. It would be ideal to distribute the noise contributions more evenly between the axes and/or reduce the contribution in the sensitive axis.

Table 3: Thruster Noise Contribution

	RSS of thruster components
X-axis	2.0
Y-axis	1.4
Z-axis	1.4

MITIGATION METHODS

A number of mitigation methods are available to address the limitations seen with the current baseline thruster configuration. Some of these methods include changing the orientation of the thrusters within the cluster and tightening the capacitive sensing and thruster noise requirements.

Thruster Orientation/Placement

Changing the thruster orientation can potentially address the concerns associated with control authority, variation levels, and noise contribution to each axis. This analysis changes the azimuth and elevation angle of the top and bottom thrusters, while the thruster location within the thruster assembly is kept constant. A number of cases are considered and the results for 12 cases are summarized in Table 4 (AO Mode) and Table 5 (SM Mode), where case #1 (45-45-135-45) is the baseline thruster configuration. In both tables, the azimuth angles are 45°, 60°, and 65° and the elevation angles are 30°, 35°, 40°, and 45°. The capabilities for the six degrees of freedom are presented and the capabilities are the same for both positive and negative values except for the z-axis force.

Attitude Only Mode (AO)

The AO mode of the DCS system has only two requirements and they are to provide coarse pointing of the spacecraft and to null any rates the spacecraft may have following the handoff from the SMART-2 controller to the ST-7 controller. Therefore, the primary criterion for determining the effectiveness of the thruster configuration in AO mode is the maximum torque available. At a minimum, the configuration must be able to counteract a 2 $\mu\text{N-m}$ torque in any axis and all the cases satisfy this requirement except for Case #9.

Table 4: Thruster Capability during Attitude Only Mode

		1	2	3	4	5	6	7	8	9	10	11	12
Azimuth (from +Z axis) of thrusters 1-2-5-6 (top)	deg	45	45	45	45	60	60	60	60	65	65	65	65
Elevation (from YZ-plane) of thrusters 1-2-5-6 (top)	deg	45	40	35	30	45	40	35	30	45	40	35	30
Azimuth (from +Z axis) of thrusters 3-4-7-8 (bottom)	deg	135	135	135	135	135	135	135	135	135	135	135	135
Elevation (from YZ-plane) of thrusters 3-4-7-8 (bottom)	deg	45	40	35	30	45	40	35	30	45	40	35	30
Maximum X Force capability (min/max thrusters at 2/20)	μN	35.3	33.9	31.8	29.0	29.5	28.5	26.8	24.4	27.3	26.4	24.9	22.8
Maximum Y Force capability (min/max thrusters at 2/20)	μN	7.9	8.6	9.2	9.7	7.9	8.6	9.2	9.7	7.0	7.5	8.1	8.5
Minimum Z Force capability (min/max thrusters at 2/20)	μN	-36.0	-39.0	-41.7	-44.1	-24.3	-26.3	-28.1	-29.7	-19.9	-21.6	-23.1	-24.4
Maximum Z Force capability (min/max thrusters at 2/20)	μN	36.0	39.0	41.7	44.1	37.2	40.3	43.1	45.5	37.6	40.7	43.6	46.1
Maximum X Torque capability (min/max thrusters at 2/20)	$\mu\text{N-m}$	2.5	2.8	2.9	3.1	2.2	2.4	2.5	2.7	1.9	2.1	2.2	2.4
Maximum Y Torque capability (min/max thrusters at 2/20)	$\mu\text{N-m}$	28.8	31.8	34.6	37.1	19.0	21.1	23.0	24.8	15.4	17.1	18.7	20.2
Maximum Z Torque capability (min/max thrusters at 2/20)	$\mu\text{N-m}$	32.4	35.1	37.5	39.7	29.3	31.7	33.9	35.9	26.8	29.0	31.1	32.8

Science Mode (SM)

The SM mode places more requirements on the thruster configuration. In particular, the configuration should allow for: the thrusters to be biased high in order to provide the largest absolute force variation given the $\pm 20\%$ constraint; equal thruster noise contribution in all axes or less thruster noise contribution in the sensitive axis; and sufficient control authority in all axes. All of this information is summarized in Table 5, where the maximum capabilities also assume that the thrusters are providing a constant 19 μN force in the +Z-direction.

As was previously stated, the baseline configuration was able to meet the performance requirements but the margins are minimal. This analysis shows a reduction in the capabilities of the X-torque to 1.2 $\mu\text{N-m}$ and Y-force capability to 4.8 μN when a constant 19 μN Z-force was required. Also, the $\pm 20\%$ thruster variation capabilities for the top and bottom thrusters are $\pm 1.7 \mu\text{N}$ and $\pm 3.6 \mu\text{N}$, respectively, for this configuration.

Table 5: Thruster Capability during Science Mode

		1	2	3	4	5	6	7	8	9	10	11	12
Azimuth (from +Z axis) of thrusters 1-2-5-6 (top)	deg	45	45	45	45	60	60	60	60	65	65	65	65
Elevation (from YZ-plane) of thrusters 1-2-5-6 (top)	deg	45	40	35	30	45	40	35	30	45	40	35	30
Azimuth (from +Z axis) of thrusters 3-4-7-8 (bottom)	deg	135	135	135	135	135	135	135	135	135	135	135	135
Elevation (from YZ-plane) of thrusters 3-4-7-8 (bottom)	deg	45	40	35	30	45	40	35	30	45	40	35	30
Maximum X Force capability (min/max thrusters at 2/20)	μN	24.0	23.7	22.5	20.5	29.5	28.5	26.8	24.4	27.3	26.4	24.9	22.7
Maximum Y Force capability (min/max thrusters at 2/20)	μN	4.8	5.7	6.4	7.1	6.1	7.1	8.0	8.8	6.5	7.6	8.6	9.5
Minimum Z Force capability (min/max thrusters at 2/20)	μN	-36.0	-39.0	-41.7	-44.1	-24.3	-26.3	-28.1	-29.7	-19.9	-21.6	-23.1	-24.4
Maximum Z Force capability (min/max thrusters at 2/20)	μN	36.0	39.0	41.7	44.1	37.2	40.3	43.1	45.5	37.6	40.7	43.6	46.1
Maximum X Torque capability (min/max thrusters at 2/20)	$\mu\text{N-m}$	1.2	1.4	1.6	1.8	1.6	1.9	2.2	2.4	1.8	2.1	2.4	2.6
Maximum Y Torque capability (min/max thrusters at 2/20)	$\mu\text{N-m}$	13.6	16.3	18.8	21.1	14.2	17.1	19.7	22.1	14.4	17.3	20.0	22.4
Maximum Z Torque capability (min/max thrusters at 2/20)	$\mu\text{N-m}$	15.3	18.0	20.4	22.6	21.9	25.6	29.0	32.0	25.1	29.3	33.1	36.4
X-axis Noise contribution (RSS of thruster components)	N/A	2.0	1.8	1.6	1.4	2.0	1.8	1.6	1.4	2.0	1.8	1.6	1.4
Y-axis Noise contribution (RSS of thruster components)	N/A	1.4	1.5	1.6	1.7	1.6	1.7	1.8	1.9	1.6	1.8	1.9	2.0
Z-axis Noise contribution (RSS of thruster components)	N/A	1.4	1.5	1.6	1.7	1.2	1.3	1.4	1.5	1.2	1.3	1.3	1.4
3-4-7-8 Thruster Bias when fighting 19 μN SRP force	μN	18	18	18	18	18	18	17.8	17.5	17.5	17.2	16.9	16.7
1-2-5-6 Thruster Bias when fighting 19 μN SRP force	μN	8.5	9.2	9.8	10.2	12.0	13.1	13.5	13.8	13.4	14.0	14.5	14.9

When considering the requirements from both the AO and SM mode, Case #12, with 30° elevation angle for all thrusters and 65° azimuth angle on the top thruster, appears to be the most favorable thruster configuration. Case #12 reduces the thruster noise contribution on the sensitive axis (X-axis), provides thruster variations of $\pm 3.3 \mu\text{N}$ and $\pm 3.0 \mu\text{N}$, and provides more torque authority ($\pm 2.6 \mu\text{N-m}$) about the X-axis while counteracting the SRP Force. The noise contribution on the sensitive axis has also been reduced with this configuration. This case assumes that plume impingement on the spacecraft is not an issue at this elevation angle. If plume impingement is an issue and the elevation angle of the thruster must be kept at 45° then Case #5 would be the configuration of choice. In AO mode, Case #5 provides 2.2 $\mu\text{N-m}$ of torque in the X-axis while in SM mode it provides $\pm 1.6 \mu\text{N-m}$ of torque in the X-axis (up $\pm 0.4 \mu\text{N-m}$ from the baseline). The available thruster variation for the top and bottom thrusters for Case

#5 are $\pm 2.4 \mu\text{N}$ and $\pm 3.6 \mu\text{N}$, respectively. The noise contribution with this configuration has slightly increased on the Y-axis but decreased on the Z-axis when compared to the baseline configuration.

Tightening the Gravitational Reference Sensor and Thruster Noise Requirements

Another factor affecting the individual thruster variation levels is the effect of the noise from both the gravitational reference sensor and the micro-Newton thrusters. Figure 14 and Figure 15 show representative root Power Spectral Density (PSD) plots of the top and bottom thruster command variations where the dominant contributors can be seen to be the capacitive sensing and thruster noise. Currently, the capacitive sensing and thruster noise requirements are modeled using a white noise model where the intensities are $3.0 \text{ nm}/\sqrt{\text{Hz}}$ and $0.1 \mu\text{N}/\sqrt{\text{Hz}}$, respectively. Refining the noise requirements to take advantage of the better than expected performance levels of the GRS sensor and thruster noise can help in reducing the individual command variations. This solution is still being investigated.

Refining the Requirements

A third possible mitigation method is to refine the spacecraft requirements. One of the current requirements placed on ST-7 requires the thrusters to counteract a $2 \mu\text{N-m}$ torque in any axis. Reducing the magnitude of this torque (for example to $0.5 \mu\text{N-m}$) provides better margins for the baseline configuration. In addition, allowing the spacecraft to fly at a zero-torque attitude (so the center of pressure-center of gravity offset can be zero) would reduce the torque requirements in SM mode.

CONCLUSION

Thruster orientation and placement is driven by three factors: thruster command variation, command authority, and noise contribution. The current thruster configuration baseline meets the performance requirements with the given operating conditions with very little margin available. Alternatives to the baseline configuration include the 60-45-135-45 case (Case #5) and the 65-30-135-30 (Case #12). The 65-30-135-30 configuration is the preferred configuration if plume impingement is not an issue since it offers for a higher minimum thruster variation ($\pm 3.0 \mu\text{N}$) in SM mode. If plume impingement is an issue, the 60-45-135-45 configuration is preferred since it allows for more thruster variation compared to the baseline and more than $2.0 \mu\text{N-m}$ torque capability in all the axes during AO mode. In addition to the modification of the thruster configuration, refining the GRS and thruster noise requirements based on better than expected performance can reduce the variations required of the thruster. The relaxation of the torque requirements on the thrusters could also improve the situation for the baseline thruster configuration. A final solution combining all mitigation methods is still being investigated.

REFERENCES

- [1] Keiser, G. M., Buchman, S., Byer, R. L., Folkner, W. M.O, Hruby, V., and Gamero-Castaño, M., "Disturbance Reduction System for Testing Technology for Drag-Free Operation," SPIE Paper 4856-02, Astronomical Telescopes and Instrumentation Conference, Waikoloa, Hawaii, USA, August 2002.

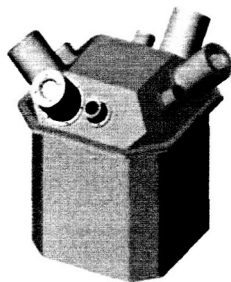
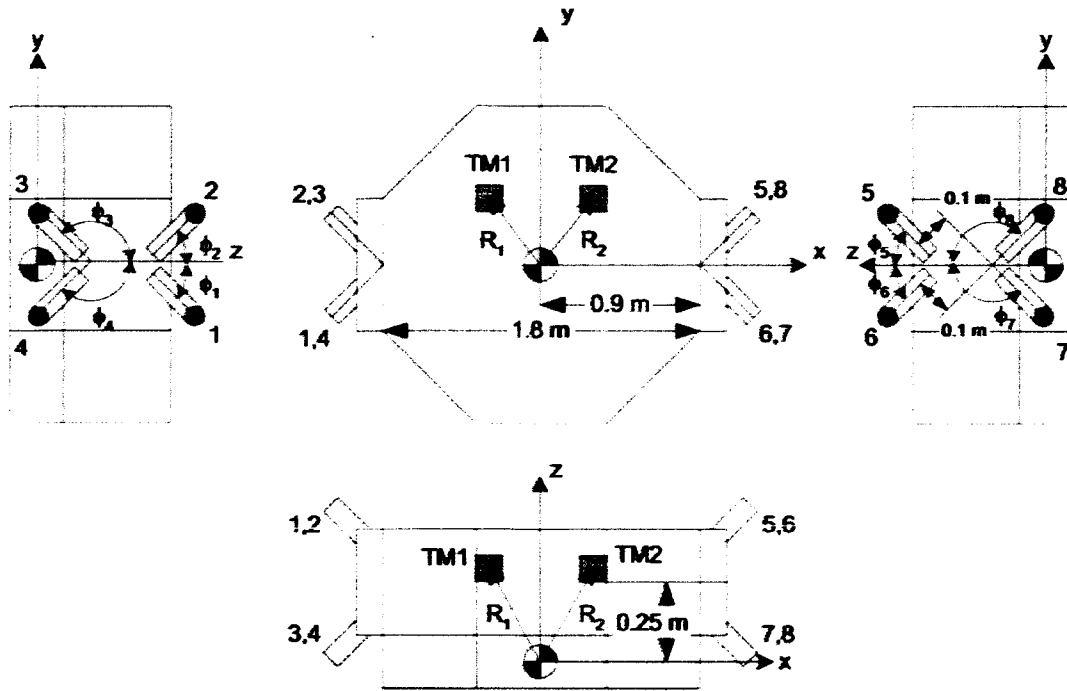


Figure 1: Perspective View of Thruster Cluster



(The elevation angle θ_m , measured from the Y-Z plane, cannot be shown in this figure.)

Figure 2: Thruster Layout and Angle Definitions

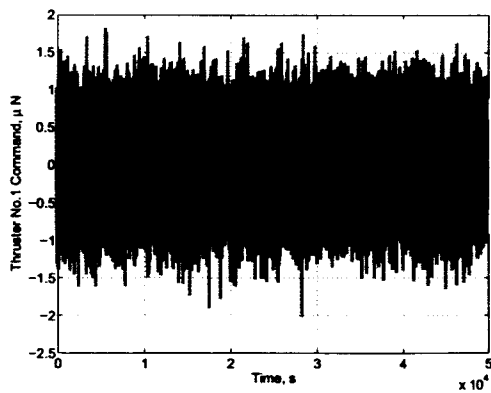


Figure 3: Thruster #1 Command Variation

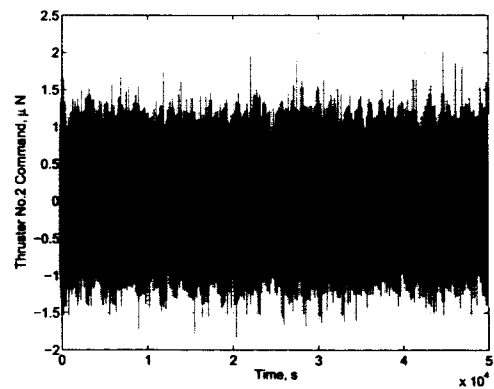


Figure 4: Thruster #2 Command Variation

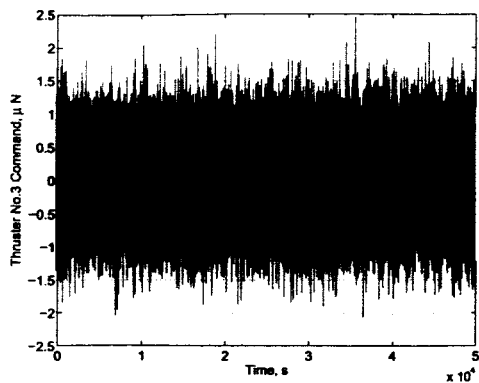


Figure 5: Thruster #3 Command Variation

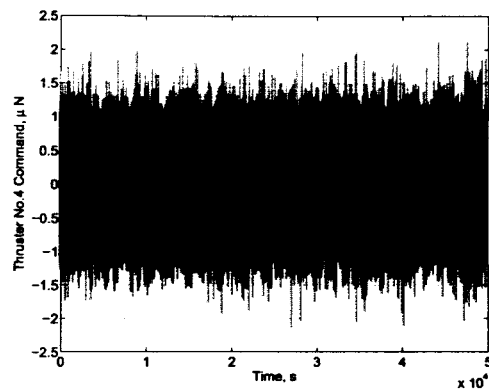


Figure 6: Thruster #4 Command Variation

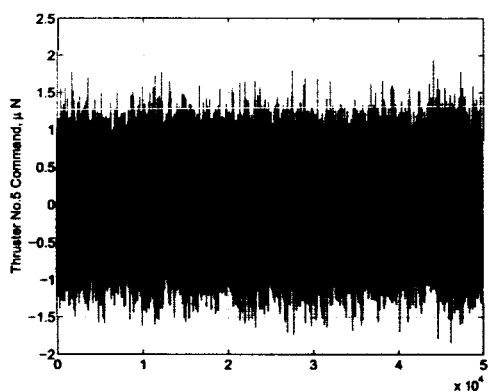


Figure 7: Thruster #5 Command Variation

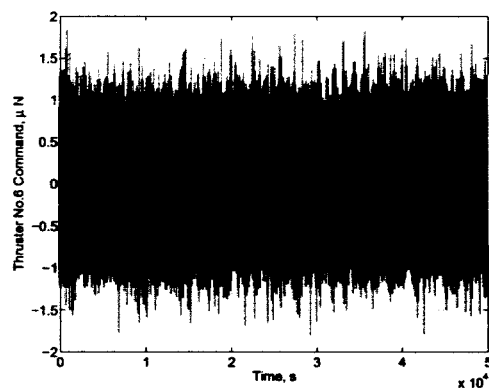


Figure 8: Thruster #6 Command Variation

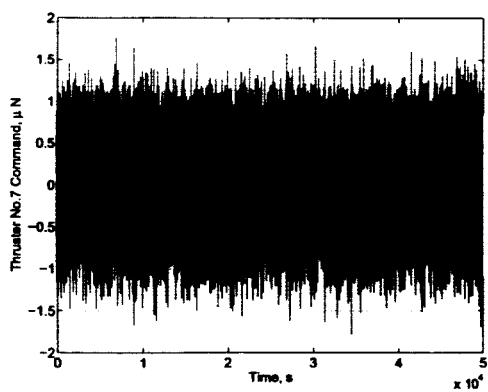


Figure 9: Thruster #7 Command Variation

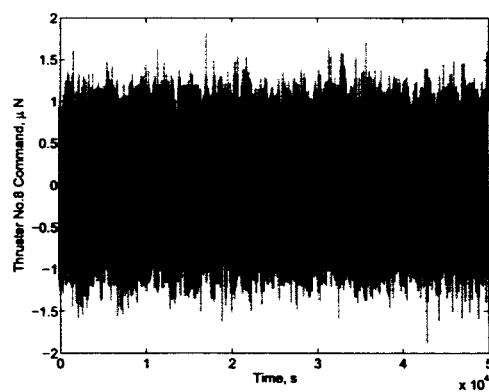


Figure 10: Thruster #8 Command Variation

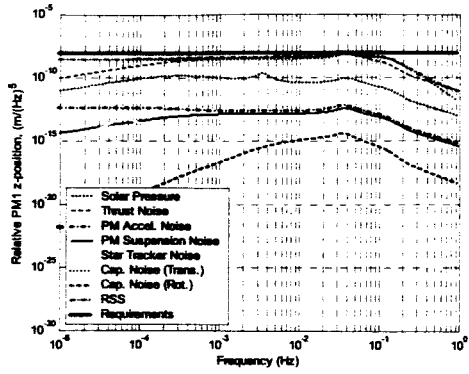


Figure 11: PSD for Gap 1 X-position

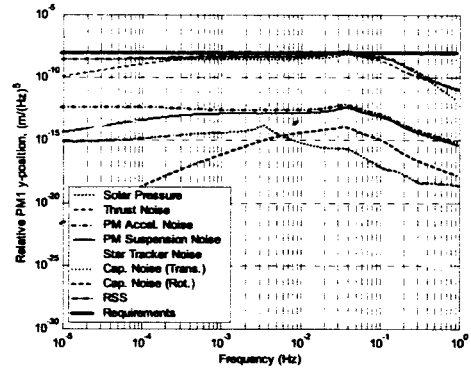


Figure 12: PSD for Gap 1 Y-position

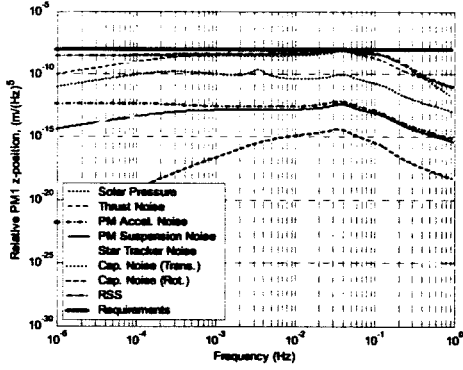


Figure 13: PSD for Gap 1 Z-position

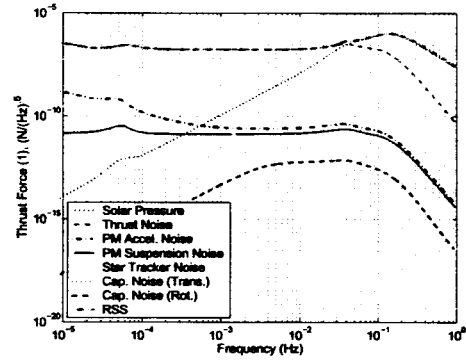


Figure 14: Thruster #1 PSD

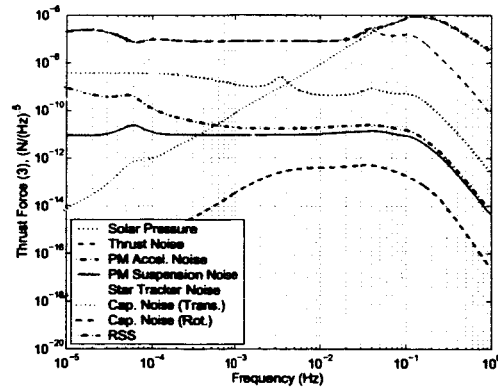


Figure 15: Thruster #3 PSD